Chapter 3

Simulating Diffraction Patterns

3.1 Introduction

Diffraction techniques provide powerful tools to study how materials order at the atomic level. X-rays were first used to probe microscopic order, these have since been supplemented with electron and neutron scattering methods. In the specific case of this work the ordered structures produced by Monte-Carlo molecular dynamic simulations can be compared to real world samples by calculating their virtual diffraction patterns for comparison with those from experiment

The study of diffraction patterns from 3-d structures is very well established. Thomas Young famously observed two slit interference of light in ~1802 concluding that light was a wave rather than a particle as proposed by Newton - a debate that still continues to this day. Such interference patterns are a natural consequence of Huygens construction where every point on a waterfront may be assumed to be a source of secondary *wavelets*. 2-d diffraction gratings were well developed by the mid 1800s. The possibility of diffraction from 3-d atomic structures was suggested by Ewald and Laue in 1912 with the first x-ray diffraction pattern produced shorty thereafter.

The terminology here is somewhat imprecise. A diffraction pattern is the result of the *interference* of *diffracted* waves. At a physical level the processes are the same, we tend to use interference when referring to a few scatterers and diffraction for many.

X-rays, electrons and neutrons are used in atomic diffraction studies. Relatively inexpensive and compact equipment is capable of generating x-rays whose wavelength is of the order of the inter-atomic spacing. X-rays scatter from electrons thus the scattering power of an atom depends upon the number of electrons it possesses i.e. its atomic number. Palladium with 46 electrons scatters much more strongly Hydrogen with only 1. In the case of Pd-H, scattering from the palladium masks the signal from the hydrogen. Instead thermal neutrons with de-Broglie wavelengths of

the order of Å s may be used as the neutron scattering factor does not vary simply with Z number and is highest for hydrogen. A suitably bright neutron source may be a nuclear reactor, such as that at Grenoble or a proton synchrotron such as ISIS which generates neutrons by spallation from a tungsten target illuminated by protons. This equipment is many times larger, expensive and complex then x-ray diffractometers. As x-ray, electron and neutron scattering patterns are due to the summing of scattered waves from the target it is straightforward to simulate this process.

A brief overview of scattering theory is first presented followed by a discussion of how a diffraction pattern may be computed from a simulated sample.

3.1.1   General Scattering Theory

The kinematic model provides a simple view of scattering. An incident wave-front may be scattered by discontinuities in its path. X-rays scatter from orbital electrons whilst neutrons scatter from atomic nuclei. These scattering centres act as sources of spherical wavefronts (*s-wave* scattering). At some distance wave-fronts from many scatterers interfere thereby creating regions of high and low intensity depending on the phase contributions from each wave.
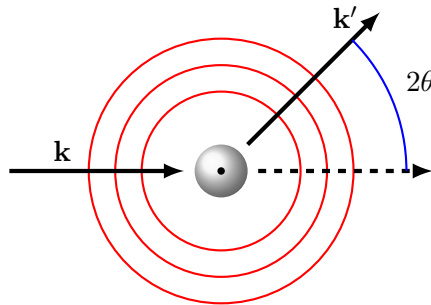

FIGURE 3.1: Simple Kinematic Scattering

In this simple treatment the scattering is assumed to be elastic i.e. the magnitude of the scattered wave vector is equal to that of the incident. $|\mathbf{k}'| = |\mathbf{k}|$. The amplitude of the incident wave arriving at a point j in the sample is given by $A_j = A_0 e^{i\mathbf{K} \cdot \mathbf{r}_j}$. Thus the scattered amplitude A_s arriving at a detector at a distance R_i from the ith atom is given by

$$A_i = \frac{A_0}{R_i} f e^{i(kx - \omega t)} \tag{3.1.1}$$

where f the scattering factor is a measure of the scattering power of the atom. If the distance to the detector is very much greater than the atomic spacing then R_i may be to a constant R. In reality a scattered wave is likely to undergo further scattering. In simple models this effect is ignored as it greatly increases computing time.

3.1.2 The Scattering Vector q

Consider two atoms i and j, illuminated by a coherent beam of radiation from a source at ∞, of wavelength λ and thus wavevector $|q| = \frac{2\pi}{\lambda}$. The difference between the incident and scattered wave vector is known as the scattering vector where $\mathbf{k}' = \mathbf{k} + \mathbf{q}$
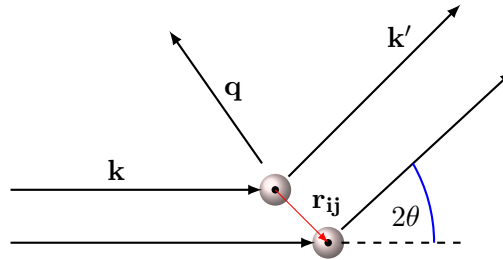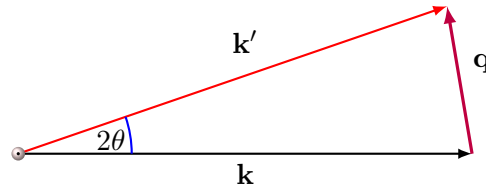
FIGURE 3.2: Wave Vectors

FIGURE 3.3: $\mathbf{k}$ incident, $\mathbf{k}'$ diffracted and $\mathbf{q}$ diffraction vectors

Given that $|\mathbf{k}'| = |\mathbf{k}|$ it is apparent that

$$|\mathbf{q}| = 2|\mathbf{k}| \sin\left(\frac{\mathbf{k}\angle\mathbf{k}'}{2}\right) \tag{3.1.2}$$

Waves incident on the detector, scattered as $\mathbf{q_i}$ and $\mathbf{q_j}$ will interfere and thus a diffraction pattern may form.

3.1.3 Formation of a Diffraction Pattern

We now imagine an ensemble of N identical atoms sitting at 3d positions $\mathbf{r_i}$ from some arbitrary origin $\mathbf{r_0}$ with a detector at a distance much greater than the size of the sample. We may thus approximate the distance from all points to the detector as a constant and ignore the amplitude-distance terms. The position of each detector pixel may be described by $\mathbf{k}'$ with respect to the origin of the sample. At some point $\mathbf{k}'$ on the detector waves scattered from the atoms arrive and interfere. The amplitude of each scattered wave is given by

$$A(\mathbf{k}') = f e^{-i(\mathbf{k}-\mathbf{k}')\cdot\mathbf{r}} \tag{3.1.3}$$
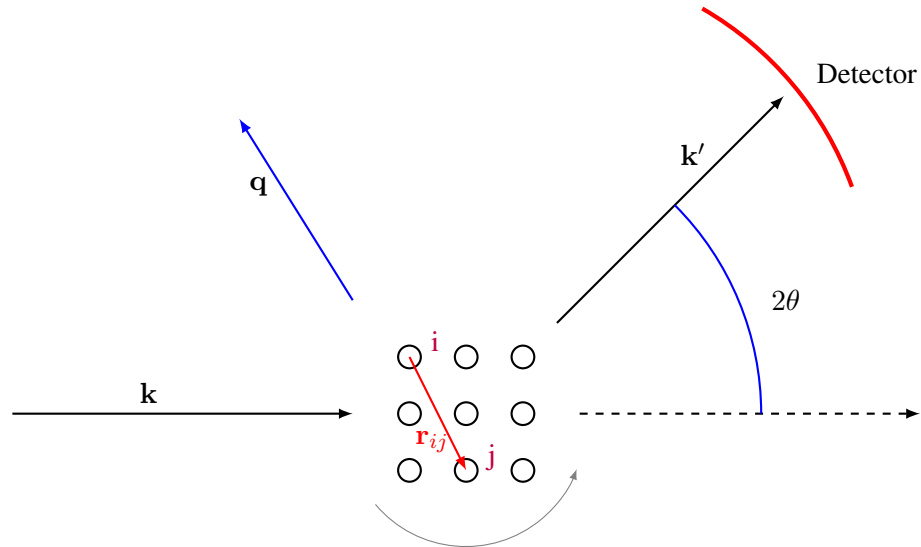
FIGURE 3.4: Diffraction pattern from many sources

As $\mathbf{q} = (\mathbf{k} - \mathbf{k}')$

$$A(\mathbf{q}) = f e^{-i(\mathbf{q} \cdot \mathbf{r})} \qquad (3.1.4)$$

For N scatterers we sum the waves from each scatterer j

$$A(\mathbf{q}) = \sum_{j=1}^{N} f_j e^{-i(\mathbf{q} \cdot \mathbf{r_j})} \qquad (3.1.5)$$

The detector will measure the intensity of the radiation at each pixel summed over all scatterers. This is equal to the square of the scattering amplitude A, being a complex number - strictly the product of the amplitude with its first complex conjugate.

$$I(\mathbf{q}) = |A||A^*| = \sum_{j=1}^{N} \sum_{k=1}^{N} b_j e^{-i \, \mathbf{q} \cdot \mathbf{r_{jk}}} \qquad (3.1.6)$$

The Bragg peaks at $n\lambda = 2d \sin \theta$ give information from long-range ordering. These simulations are concerned with short-range order resulting from growth of crystal domains. The size of domains may be inferred from their broadening of the Bragg peaks using the Scherrer equation

$$\tau = \frac{K\lambda}{\beta \sin \theta} \qquad (3.1.7)$$

where τ is the domain size, K a dimensionless shape parameter generally taken as 0.9. β is the full width - half maximum peak broadening expressed in radians and θ the Bragg angle. ****
image of peak broadening *******

3.1.4 Pair Distribution Functions

The diffraction pattern is a function of the degree of spacial ordering within the sample therefore of the density distribution of scatterers. Taking into account such pair distribution is of particular importance when considering partly ordered systems.

The reduced P.D.F. $g(r)$ is simply the probability of finding a pair of particles at a specific distance r from one another. $g(r)$ is often expressed as the normalised form such that as $r \to \infty, g(r) \to 1$ and for $r <$ distance of closest approach $g(r) = 0$. The pair distribution function may be obtained directly from a M.D. simulation where it is related to the pair density function $\rho(r)$ by $\rho(r) = \rho_0 g(r)$. As $r \to \infty$, $\rho(r)$ will tend to ρ_0, the mean number density of the sample and tend to zero as $r \to 0$

$$g(r) = 4\pi r \left(\rho(r) - \rho_0\right) = 4\pi \rho_0 r \left(g(r) - 1\right) \tag{3.1.8}$$

Within a shell at a range $r_1 \to r_2$ we may specify the number of neighbours, a site's coordination number as

$$N_c = \int_{r_1}^{r_2} R(r)\, dr \tag{3.1.9}$$

In the Debye scattering method the calculation is optimised by 'binning' these coordination numbers in advance then calculating

$$I(q) = \frac{1}{N} \sum_{i=1}^{N} f_i N_{c_i} \frac{sin(2\pi q r_i)}{2\pi q r_i} \tag{3.1.10}$$
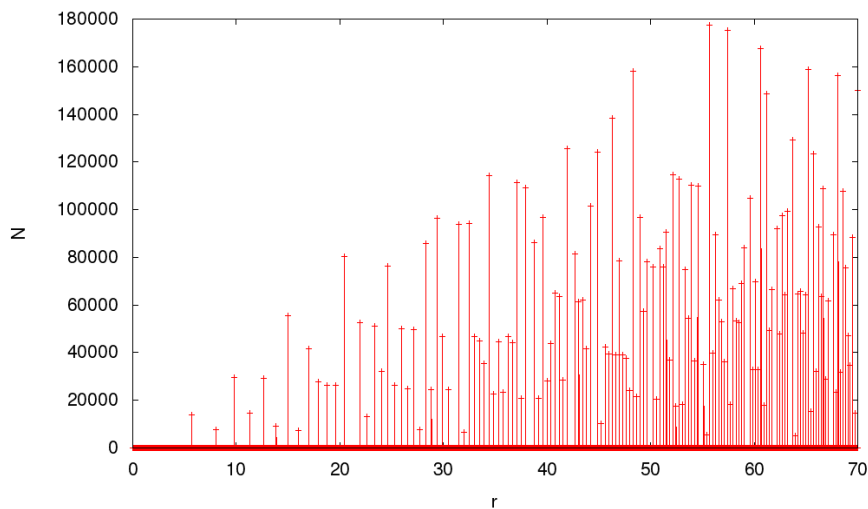

FIGURE 3.5: Example of binned interatomic distances for C=0.29 ordered lattice

We may now specify a radial distribution function $R(r)$ describing the number of atoms in a shell of thickness $d(r)$ at a distance r:-

$$R(r) = 4\pi r^2 \rho(r) \qquad (3.1.11)$$

giving

$$g(r) = \frac{R(r)}{r} - 4\pi r \rho_0 \qquad (3.1.12)$$

This may be easily determined at any point in a molecular dynamics simulation. If we assume initially that atoms sit at precise positions $\mathbf{r_i}$ without thermal or other displacements then their positions may be expressed as a series of delta functions $\delta(\mathbf{r_0} - \mathbf{r_i})$. Setting $\mathbf{r_0} = 0$ gives

$$R(r) = \frac{1}{N} \sum_i \sum_j \delta(\mathbf{r_{ij}}) \qquad (3.1.13)$$

The reduced pair distribution function $g(r)$ is the Fourier Transform of $S(q)$ the total scattering structure function – effectively the normalised diffraction pattern.

$$G(r) = \frac{2}{\pi} \int_{qmin}^{qmax} q[S(\mathbf{q}) - 1]sin(qr)dq \qquad (3.1.14)$$

The inverse transform is more useful here

$$S(q) = 1 + \frac{1}{q} \int_0^\infty r(r)sin(qr)dr \qquad (3.1.15)$$

3.1.5 The Role of Reciprocal Space

Reciprocal space (also *momentum space, k-space* is a convenient abstraction when considering diffraction from a periodic structure being the Fourier transform of the real space *direct* lattice. Points in reciprocal space represent families of planes in the direct lattice. A key feature being that the vector direction between any two point in the reciprocal lattice represents the direction between two planes in the direct lattice. The magnitude of the reciprocal vector is the reciprocal of the interplanar spacing. Expressing these reciprocal lattice vector lengths as $|\mathbf{G}| = \frac{2\pi}{\lambda}$ gives the distance in radians per unit length.

If we have a set of atomic positions in real space $\mathbf{r_i} = (h\mathbf{x_i} + k\mathbf{y_i} + l\mathbf{z_i})$ then the Fourier transform is given by

$$f(\mathbf{r}) = \sum_G f(\mathbf{G})e^{i(\mathbf{G} \cdot \mathbf{r})} \qquad (3.1.16)$$

The key point here is that this transform maps directly the diffraction pattern from the scatterers i.e.

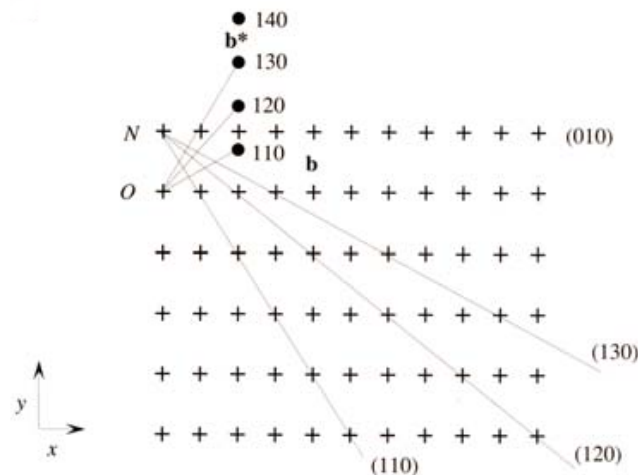$$S(\mathbf{q}) = \sum_{i,j,k} e^{i\mathbf{G}\cdot\mathbf{r}} \tag{3.1.17}$$

FIGURE 3.6: Construction of the Reciprocal Lattice.

Real space points are +, reciprocal points ·

The reciprocal lattice axis vectors are given by

$$\mathbf{b}_1 = 2\pi \frac{\mathbf{a}_2 \times \mathbf{a}_3}{\mathbf{a}_1 \cdot \mathbf{a}_2 \times \mathbf{a}_3} \qquad \mathbf{b}_2 = 2\pi \frac{\mathbf{a}_3 \times \mathbf{a}_1}{\mathbf{a}_1 \cdot \mathbf{a}_2 \times \mathbf{a}_3} \qquad \mathbf{b}_3 = 2\pi \frac{\mathbf{a}_1 \times \mathbf{a}_2}{\mathbf{a}_1 \cdot \mathbf{a}_2 \times \mathbf{a}_3} \tag{3.1.18}$$

Note that $\mathbf{b}_1$ is orthogonal to both $\mathbf{a}_2$ and $\mathbf{a}_3$, $\mathbf{b}_2$ is to both $\mathbf{a}_1$ and $\mathbf{a}_3$ and so on. Points in the reciprocal lattice are mapped as

$$\mathbf{G} = h\mathbf{b}_1 + k\mathbf{b}_2 + l\mathbf{b}_3 \tag{3.1.19}$$

As is generally accepted diffraction peaks occur when $\mathbf{q} = \mathbf{G}$. [70]

3.2 Simulating a Diffraction Pattern

Given a known crystal structure one may calculate the reflections from specific planes - the inverse of conventional experimental crystallography. The alternate approach, used here is to calculate the diffraction pattern from a set of atomic positions mirroring the physical processes in experimental x-ray or neutron crystallography. Such an *a priori* technique makes few of the

assumptions of conventional crystallography such as 'reflection from planes' though is computationally somewhat expensive. Since we are considering an *a priori* algorithm it may be helpful to initially limit standard crystallographic terminology and formulate the problem in general physical terms.

We wish to simulate the diffraction pattern formed when a beam of radiation is incident upon group of atoms. These scatterers interact with the incident radiation resonating and emitting spherical wavefronts. Different scatterers will have different scattering powers. Here we are only considering scattering by Hydrogen so this scattering *factor* can be set to unity. A number of methods have been developed to simulate diffraction patterns directly from atomistic data.

The most direct takes a rather *brute force* approach. One simply determines the linear path lengths from a monochromatic coherent radiation source to each atom in the model and from there to every pixel on the detector array . Sin 2π and cos 2π of $n\lambda$ for each path are summed at each pixel giving the resultant amplitude and phase. This scales directly with $N_{atoms} \times n_{pixels}$, for a sample of 10^6 atoms and a linear detector of 10^4 pixels one has of the order of 10^{10} iterations - perfectly acceptable on a modern workstation. Since each calculation does not depend on the others then this is easily optimised by parallel processing. One problem here though is the need for the paths lengths to be very long compared to the size of the sample and hence the differences in atomic positions. This to avoid distortion of the pattern by some parts of the sample being significantly closer to the detector than others. If the simulation mirrors a real diffractometer the sample $\rightarrow$ detector distance will be $> 10^8\times$ the inter-atomic spacing. Assuming that we need to resolve path differences of 10^{-2} of this spacing we require a precision of $1 : 10^{10}$. To overcome this one needs to use high precision 'long' real numbers which significantly slows computation.

A more sophisticated approach involves calculating

$$I(\mathbf{k}') = \sum_{i \neq j} \sum_{j} e^{i\mathbf{q}\cdot\mathbf{r}_{ij}} \tag{3.2.1}$$

to every point on the detector array (fig: 3.4). If we assume that to the incoming radiation each atom acts as a point scatterer and that the atoms do not move their positions may be represented as a series of δ-functions. A further simplification may be introduced in assuming that the size of the region being sampled is much smaller than the distance between the sample and the detector. Thus we can assume that the scattering distance and angle from each atom to each point on the detector are approximately constant. The problem with this method again computational load. For a sample of 10^5 atoms and a 2d detector of 10^6 pixels one would need to perform some 10^{16} calculations before needing to rotate the sample to ensure that all possible peaks are detected. Without optimisation this is impractical. This has the appearance of Fourier transform and so it should be practical to perform an F.F.T. if we assume that the scatterers are both point entities

and sit on points fixed on a regular 3d lattice. If the points are permitted to displace from these regular point, via thermal vibration or during diffusion one cannot perform an FFT. This could be addressed by defining a grid whose spacing is much smaller than the lattice parameter and limiting scatters to these discrete positions. With say 10^6 atoms and 10 intermediate points between the *regular* lattice sites results a grid of 10^9 points with only 0.1% filled at any time. This will lead to very large data arrays which without some optimisation will again add to computation time.

In the 1980s a simulation technique using the Debye scattering equation for powder samples was developed.

$$I(q) = \frac{1}{N} \sum_{i=1}^{N} \sum_{j=1}^{N} f_i f_j \frac{sin(2\pi q r_{ij})}{2\pi q r_{ij}} \qquad (3.2.2)$$

where f_i, f_j are the scattering factors of the respective atoms and q, r_{ij} are equal to $|\mathbf{q}|$ and $|\mathbf{r_{ij}}|$ respectively. The algorithm may be optimised by binning the distances r_{ij} before performing
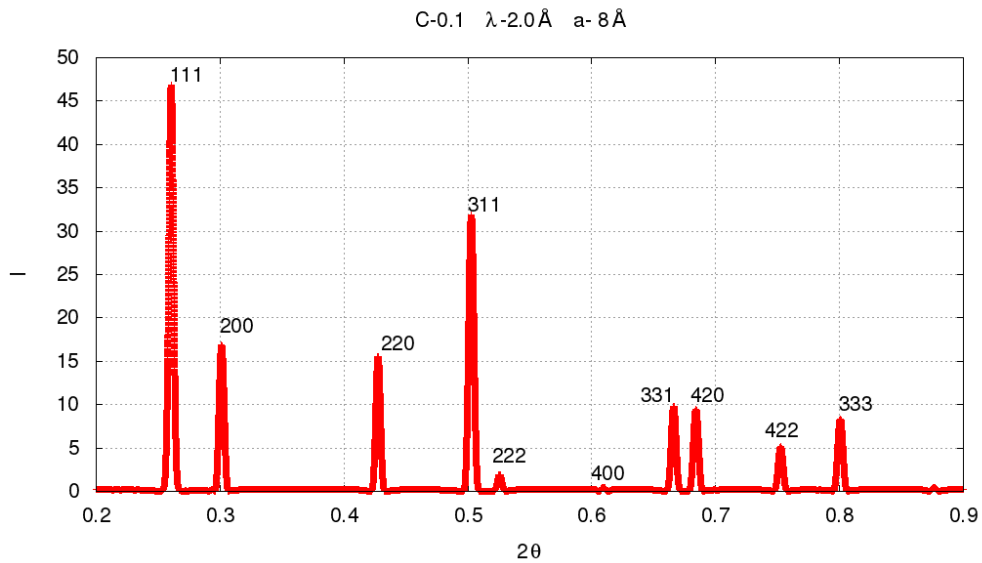

FIGURE 3.7: Virtual Debye Diffraction Pattern demonstrating only (hkl) all odd or all even as expected for FCC structure

the computational intensive sin calculations. With sufficiently narrow bins errors generated are minimal (fig (3.5). In effect this technique loses the absolute spacial, i.e. directional, information in favour of computationally faster method of generating pair distributions (the bins). The size of crystal regions may be inferred from peak broadening rather than being directly observed. This technique is very fast, on a 3 GHz workstation a pattern from 10^4 atoms, with 10^4 detector pixels and 10^5 bins computes in some 100 seconds(fig 3.7). Scaling to a more realistic 10^6 atoms takes $\sim$ 3 hours.

The technique used here for the contour 2d plots involves summing $e^{i(\mathbf{G}\cdot\mathbf{r}_i)}$ over a range of G_x and G_y (fig 3.8).
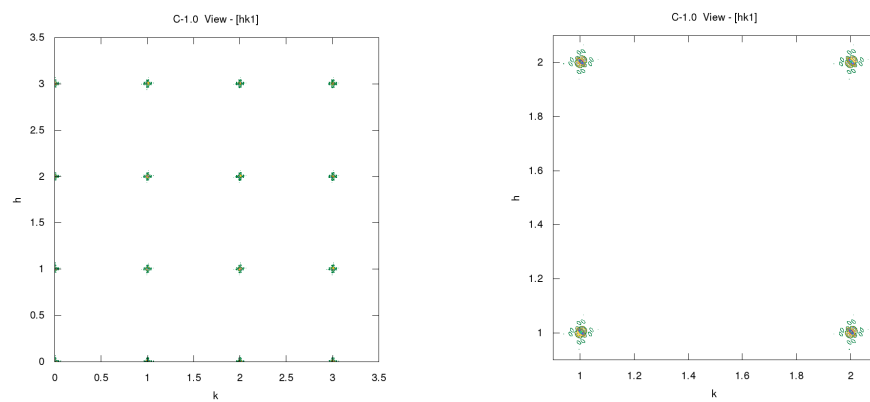
FIGURE 3.8: 2d contour plots of partly filled lattice in (hk1)

Bibliography

[1] T. Abbas, M. Ullah, A. M. Rana, and R. M. Arif-Khalil. Calculation of short range order in nirh, nipd and curh alloys. *Materials Science-Poland, Vol. 25, No. 4*, 2007.

[2] G J Ackland. Calculation of free energies from ab initio calculation. *Journal of Physics: Condensed Matter*, 14(11):2975, 2002.

[3] B. Andreev. Separation of hydrogen isotopes by chemical isotope exchange in systems involving metal and intermetallic compound hydrides. *Separation Science and Technology*, 2001.

[4] B. Andreyev, V. Shitikov, E. Magomedbekov, and A. Shafiev. Isotopic effects in hydrogen-intermetallic compound systems. *Journal of the Less Common Metals*, 90(2):161 – 168, 1983.

[5] V. E. Antonov, A. I. Davydov, V. K. Fedotov, A. S. Ivanov, A. I. Kolesnikov, and M. A. Kuzovnikov. Neutron spectroscopy of h impurities in pdd: Covibrations of the h and d atoms. *Phys. Rev. B*, 80:134302, Oct 2009.

[6] Ralph Baierlein. The elusive chemical potential. *American Journal of Physics*, 69(4):423–434, 2001.

[7] I S Balbaa and F D Manchester. Superconductivity of pdh x in relation to its phase diagram. i. magnetic measurements. *Journal of Physics F: Metal Physics*, 13(2):395, 1983.

[8] I S Balbaa, A J Pindor, and F D Manchester. Superconductivity of pdh x in relation to its phase diagram. ii. specific heat measurements and the form of the t c (x) relaxation. *Journal of Physics F: Metal Physics*, 14(11):2637, 1984.

[9] J Barber. Simulation of x-ray diffraction patterns. *Los Alamos National Laboratory*, 2010.

[10] R Bass, W A Oates, H R Schober, and A M Stoneham. Configuration-independent elastic interactions in metal-hydrogen solutions. *Journal of Physics F: Metal Physics*, 14(12):2869, 1984.

[11] S.Z. Baykara. Theoretical evaluation of diffusivity of hydrogen in palladium and rhodium. *International Journal of Hydrogen Energy*, 29(15):1631 – 1636, 2004.

[12] W Betteridge and J Hope. The separation of hydrogen from gas mixtures. *Platinum Metals Review*, 1975.

[13] K Beyerlein. *Simulation of the Powder Diffraction pattern from Nanoparticles - Studying the Influence of Surface Strain*. PhD thesis, Georgia Institute of Technology, 2011.

[14] Simon J.L. Billinge. Nanoscale structural order from the atomic pair distribution function (pdf): There's plenty of room in the middle. *Journal of Solid State Chemistry*, 181(7):1695 – 1700, 2008. Solid State Chemistry on the Nanoscale: Achievements, Challenges, and Opportunities.

[15] K. Binder. Ordering of the face-centered-cubic lattice with nearest-neighbor interaction. *Phys. Rev. Lett.*, 45:811–814, Sep 1980.

[16] K. Binder. Monte carlo study of entropy for face-centered cubic ising antiferromagnets. *Zeitschrift fr Physik B Condensed Matter*, 45(1):61–69, 1981.

[17] K Binder. Applications of monte carlo methods to statistical physics. *Reports on Progress in Physics*, 60(5):487, 1997.

[18] Andreas Blomqvist, Gunnar K. Pálsson, C. Moysés Araújo, Rajeev Ahuja, and Björgvin Hjörvarsson. Significance of self-trapping on hydrogen diffusion. *Phys. Rev. Lett.*, 105:185901, Oct 2010.

[19] R A Bond and D K Ross. The use of monte carlo simulations in the study of a real lattice gas and its application to the alpha ' pd-d system. *Journal of Physics F: Metal Physics*, 12(4):597, 1982.

[20] F. M. Bulnes, V. D. Pereyra, and J. L. Riccardo. Collective surface diffusion: n-fold way kinetic monte carlo simulation. *Phys. Rev. E*, 58(1):86–92, Jul 1998.

[21] Burch. The form of the interaction between hydrogen and palladium.pdf. *Platinum Metals Rev., 1971*, 1971.

[22] Alessio Caravella, Francesco Scura, Giuseppe Barbieri, and Enrico Drioli. Sieverts law empirical exponent for pd-based membranes: Critical analysis in pure h2 permeation. *The Journal of Physical Chemistry B*, 114(18):6033–6047, 2010.

[23] S. Chen, M. Lee, K.H. Zhao, and Gary D. Doolen. A lattice gas model with temperature. *Physica D: Nonlinear Phenomena*, 37(13):42 – 59, 1989.

[24] O. B. Christensen, P. D. Ditlevsen, K. W. Jacobsen, P. Stoltze, O. H. Nielsen, and J. K. No/rskov. H-h interactions in pd. *Phys. Rev. B*, 40:1993–1996, Jul 1989.

[25] Philip C. Clapp and S. C. Moss. Correlation functions of disordered binary alloys. ii. *Phys. Rev.*, 171:754–763, Jul 1968.

[26] Philip C. Clapp and Simon C. Moss. Correlation functions of disordered binary alloys. i. *Phys. Rev.*, 142:418–427, Feb 1966.

[27] S P Coleman, D E Spearot, and L Capolungo. Virtual diffraction analysis of ni [010] symmetric tilt grain boundaries. *Modelling and Simulation in Materials Science and Engineering*, 21(5):055020, 2013.

[28] M. Cyrott, F. Cyrot-Lackmann, Desjonquères, M. C., and J.P. Gaspard. Effect of short range order on the electronic structure of disordered transition alloys. *J. Phys. Colloques*, 38(C7):C7–285–C7–288, 1977.

[29] Nicholas D. Deveau, Yi Hua Ma, and Ravindra Datta. Beyond sieverts' law: A comprehensive microkinetic model of hydrogen permeation in dense metal membranes. *Journal of Membrane Science*, 437(0):298 – 311, 2013.

[30] H. T. Diep, A. Ghazali, B. Berge, and P. Lallemand. Phase diagrams in f.c.c. binary alloys: Frustration effects. *EPL (Europhysics Letters)*, 2(8):603, 1986.

[31] S. Dietrich and H. Wagner. Model calculation for the incoherent phase-transition in the palladium-hydrogen system. *Zeitschrift fr Physik B Condensed Matter*, 36(2):121–126, 1979.

[32] M. L. Doyle and I. R. Harris. Palladium rare earth alloys, their order disorder transformations and behaviour with hydrogen. *Unknown Journal*, 1988.

[33] B Dunlap, R Brenner, R Mowrey, J Mintmire, and C White. Linear combination of gaussian-type orbitals local-density-functional cluster studies of d-d interactions in titanium and palladium. *Physical Review B*, 1990.

[34] Y Ebisuzaki and M Kass, W andO'Keeffe. Solubility and diffusion of hydrogen and deuterium in platinum. *Journal of Chemical Physics*, 1968.

[35] TE Ellis, CB Sattherthwaite, MH Mueller, and TO Brun. Evidence for h (d) ordering in pdhx (pddx). *Physical review letters*, 42(7):456–458, 1979.

[36] C. Elsaasser, M. Fähnle, L. Schimmele, C. T. Chan, and K. M. Ho. Range of forces on host-metal atoms around interstitial hydrogen in pd and nb. *Phys. Rev. B*, 50:5155–5159, Aug 1994.

[37] C. Elsasser, M. Fhnle, K.M. Ho, and C.T. Chan. Ab initio pseudopotential calculations of total energies and forces for hydrogen in palladium. *Physica B: Condensed Matter*, 172(12):217 – 224, 1991.

[38] C Elsasser, KM HO, CT Chan, and M Fahnle. Vibrational states for hydrogen in palladium. *Physical Review B*, 44(18):10377–10380, NOV 1 1991.

[39] J. Evans, I.R. Harris, and D.K. Ross. A proposed method of hydrogen isotope separation using palladium alloy membranes. *Journal of the Less Common Metals*, 89(2):407 – 414, 1983.

[40] Fernandes, jeferson, Arenzon, and Levin. Monte carlo simulations of two-dimensional hard core lattice gases. *The Journal of Chemical Physics*, 2006.

[41] T B Flanagan and W A Oates. The palladium-hydrogen system. *Annual Review of Materials Science*, 21(1):269–304, 1991.

[42] T.B. Flanagan and Y. Sakamoto. Hydrogen in disordered and ordered palladium alloys. *International Journal of Hydrogen Energy*, 19(2):151 – 159, 1994.

[43] Ted B. Flanagan, W. Luo, and J.D. Clewley. Calorimetric enthalpies of absorption and desorption of protium and deuterium by palladium. *Journal of the Less Common Metals*, 172174, Part A(0):42 – 55, 1991.

[44] D. De Fontaine. Configurational thermodynamics of solid solutions. volume 34 of *Solid State Physics*, pages 73 – 274. Academic Press, 1979.

[45] D. De Fontaine. Cluster approach to order-disorder transformations in alloys. volume 47 of *Solid State Physics*, pages 33 – 176. Academic Press, 1994.

[46] Satoshi Fukada, Katsuhiro Fuchinoue, and Masabumi Nishikawa. Isotope separation factor and isotopic exchange rate between hydrogen and deuterium of palladium. *Journal of nuclear materials*, 226(3):311–318, 1995.

[47] B. Fultz. Vibrational thermodynamics of materials. *Progress in Materials Science*, 2012.

[48] Josiah Willard Gibbs. *Scientific Papers of J. Willard Gibbs p418*. Longmans, Green and Co., 1906.

[49] M J Gillan. A simulation model for hydrogen in palladium. i. single-particle dynamics. *Journal of Physics C: Solid State Physics*, 19(31):6169, 1986.

[50] M J Gillan. A simulation model for hydrogen in palladium. ii. mobility and thermotransport. *Journal of Physics C: Solid State Physics*, 20(4):521, 1987.

[51] Axel Gro. Ab initio molecular dynamics simulations of the adsorption of h2 on palladium surfaces. *ChemPhysChem*, 11(7):1374–1381, 2010.

[52] Satoshi Hata, Syo Matsumura, Noriyuki Kuwano, and Kensuke Oki. Short range order and its transformation to long range order in ni4mo. *Acta Materialia*, 46(3):881 – 892, 1998.

[53] Satoshi Hata, Syo Matsumura, Noriyuki Kuwano, and Kensuke Oki. Short range order and its transformation to long range order in ni4mo. *Acta Materialia*, 46(3):881 – 892, 1998.

[54] F. J. Higuera and J. Jimnez. Boltzmann approach to lattice gas simulations. *EPL (Europhysics Letters)*, 9(7):663, 1989.

[55] H Horner and H Wagner. A model calculation for the alpha-alpha' phase transition in metal-hydrogen systems. *Journal of Physics C: Solid State Physics*, 7(18):3305, 1974.

[56] D. K. Hsu and R. G. Leisure. Elastic constants of palladium and beta-phase palladium hydride between 4 and 300 k. *Phys. Rev. B*, 20:1339–1344, Aug 1979.

[57] Karl K. Irikura. Experimental vibrational zero-point energies: Diatomic molecules. *Journal of Physical and Chemical Reference Data, Volume 36, Issue 2, pp. 389-397*, 38(3):749–749, 2007.

[58] L.E. Isaeva, D.I. Bazhanov, E.I. Isaev, S.V. Eremeev, S.E. Kulkova, and I.A. Abrikosov. Dynamic stability of palladium hydride: An ab initio study. *International Journal of Hydrogen Energy*, 36(1):1254 – 1258, 2011.

[59] Borg R J and J Dienes G. *An Introduction to Solid State Diffusion*. 1988.

[60] J K Jacobs and F D Manchester. The 50k transition in palladium hydrogen alloys. ii. specific heat and thermal relaxation. *Journal of Physics F: Metal Physics*, 7(1):23, 1977.

[61] J.K. Jacobs and F.D. Manchester. Thermal and motional aspects of the 50 k transition in pdh and pdd. *Journal of the Less Common Metals*, 49(0):67 – 73, 1976.

[62] HC Jamieson, GC Weatherly, and FD Manchester. Beta-alpha-phase transformation in palladium-hydrogen alloys. *Journal of the Less Common Metals*, 50(1):85–102, 1976.

[63] E T Jaynes. Gibbs vs boltzmann entropies. *American Journal of Physics*, 33(5):391, 1965.

[64] J.-M. Joubert and S. Thiebaut. Thermodynamic description of the pd-h-d-t system. *J of Nuclear Materials*, 59(4):1680 – 1691, 2009.

[65] J. Kanamori and Y. Kakehashi. Conditions for the existence of ordered structure in binary alloy systems. *Journal de Physique Colloques 38*, 1977.

[66] H. Katsuta, R.J. Farraro, and R.B. McLellan. The diffusivity of hydrogen in palladium. *Acta Metallurgica*, 27(7):1111 – 1114, 1979.

[67] S W Kelly and C A Sholl. Theory and monte carlo calculation of the tracer correlation factor. *Journal of Physics C: Solid State Physics*, 20(32):5293, 1987.

[68] M. Kemali, J. E. Totolici, D. K. Ross, and I. Morrison. Inelastic neutron scattering measurements and ab initio calculations of hydrogen in single-crystal palladium. *Phys. Rev. Lett.*, 84:1531–1534, Feb 2000.

[69] A. Kerrache, H. Bouzara, M. Zemirli, V. Pierron-Bohnes, M. C. Cadeville, and M. A. Khan. Monte-carlo simulation of order-disorder kinetics in 2d and fcc binary alloys. *Computational Materials Science*, 17(2-4):324 – 330, 2000.

[70] Charles Kittel. *Introduction to Solid State Physic 8th Edition*. Wiley, 2005.

[71] Piotr Kowalczyk and J. M. D. MacElroy. Equilibrium properties of dense hydrogen isotope gases based on the theory of simple fluids. *The Journal of Physical Chemistry B*, 110(30):14971–14975, 2006.

[72] T Kuji, W A Oates, B S Bowerman, and T B Flanagan. The partial excess thermodynamic properties of hydrogen in palladium. *Journal of Physics F: Metal Physics*, 13(9):1785, 1983.

[73] U.D. Kulkarni. Monte carlo simulation of ordering transformations in nimo-based alloys. *Acta Materialia*, 52(9):2721 – 2732, 2004.

[74] Hitoshi Kurokawa, Taku Nakayama, Yasunori Kobayashi, Ken Suzuki, Mutsumi Takahashi, Seiichi Takami, Momoji Kubo, Naotsugu Itoh, Parasuraman Selvam, and Akira Miyamoto. Monte carlo simulation of hydrogen absorption in palladium and palladium-silver alloys. *Catalysis Today*, 82:233 – 240, 2003.

[75] J. R. Lacher. The statistics of the hydrogen-palladium system. *Mathematical Proceedings of the Cambridge Philosophical Society*, 33:518–523, 9 1937.

[76] J R Lacher. A theoretical formula for the solubility ofhydrogen in palladium. *Proc. R. Soc. Lond*, 1937.

[77] R. Lasser. Palladium-tritium system. *Phys. Rev. B*, 26:3517–3519, Sep 1982.

[78] R. Lasser. Solubility of protium, deuterium, and tritium in the alpha phase of palladium. *Phys. Rev. B*, 29:4765–4768, Apr 1984.

[79] R. Lasser and K Klatt. Solubility of hydrogen isotopes in palladium. *Phys. Rev. B*, 28(2):748–758, Jul 1983.

[80] R. Lasser and G. L. Powell. Solubility of h, d, and t in pd at low concentrations. *Phys. Rev. B*, 34:578–586, Jul 1986.

[81] F.A. Lewis. The palladium-hydrogen system a survey of hydride formation and the effects of hydrogen contained within the metal lattices. *Platinum Metals Review*, 1982.

[82] Y. Lin. *Atomistic modeling of nano-materials: From classical to ab initio simulations in different timescales.* PhD thesis, Rice University, 2008.

[83] Tengfei Luo and John R. Lloyd. Grand canonical monte carlo simulation of hydrogen adsorption in different carbon nano structures. *International Journal of Energy for a Clean Environment*, 10(1-4):37–56, 2009.

[84] Weifang Luo, Donald Cowgill, and Ted B. Flanagan. Separation factors for hydrogen isotopes in palladium hydride. *The Journal of Physical Chemistry C*, 0(ja):null, 2013.

[85] S. Majorowski and B. Baranowski. Diffusion coefficients of hydrogen and deuterium in highly concentrated palladium hydride and deuteride phases. *Journal of Physics and Chemistry of Solids*, 43(12):1119 – 1127, 1982.

[86] F.D. Manchester. Lattice gas aspects of metal-hydrogen system. *Journal of the Less Common Metals*, 49(0):1 – 12, 1976. Hydrogen in metals.

[87] W. Maysenholder. On the determination of interaction parameters from correlations in binary alloys. *physica status solidi (b)*, 139(2):399–408, 1987.

[88] B. C. McAlister and B. P. Grady. Simulation of small-angle x-ray scattering from single-particle systems. *Journal of Applied Crystallography*, 31(4):594–599, Aug 1998.

[89] R. A. McKee. Site blocking and correlated defect motion in tracer and chemical diffusion. *Phys. Rev. B*, 21:4269–4281, May 1980.

[90] K. G. McLennan, E. MacA. Gray, and J. F. Dobson. Deuterium occupation of tetrahedral sites in palladium. *Physical Review B*, 78(1), JUL 2008.

[91] H Meirovitch. Methods for estimating entropy with computer simulation: the simple cubic ising lattice. *Journal of Physics A: Mathematical and General*, 16(4):839, 1983.

[92] Hagai Meirovitch. Computer simulation study of hysteresis and free energy in the fcc ising antiferromagnet. *Phys. Rev. B*, 30:2866–2874, Sep 1984.

[93] N. Metropolis, A.W. Rosenbluth, M.N. Rosenbluth, A.H. Teller, and E. Teller. Equations of state calculations by fast computing machines. *Journal of Chemical Physics*, 1953.

[94] T Mohri and W Oates. Cvm-based calculation of the p d-h phase diagram in the high temperature region. *Material Transactions V13*, 2002.

[95] T Mohri and W.A Oates. Theoretical investigation of pdh phase equilibria by the cluster variation method. *Journal of Alloys and Compounds*, 330332(0):14 – 19, 2002. Proceedings of the International Symposium on Metal-Hydrogen Systems, Fundamentals and Applications (MH2000).

[96] S. C. Moss and Philip C. Clapp. Correlation functions of disordered binary alloys. iii. *Phys. Rev.*, 171:764–777, Jul 1968.

[97] M. Muller and J.J. de Pablo. Simulation techniques for calculating free energies. In Mauro Ferrario, Giovanni Ciccotti, and Kurt Binder, editors, *Computer Simulations in Condensed Matter Systems: From Materials to Chemical Biology Volume 1*, volume 703 of *Lecture Notes in Physics*, pages 67–126. Springer Berlin Heidelberg, 2006.

[98] S. Muller. First-principles based multiscale modelling of alloys. *Multiscale Simulation Methods in Molecular Science*, 2009.

[99] G.E. Murch and R.J. Thorn. Computer simulation of the chemical potential. *Conference on computer simulation for materials applications*, 1976.

[100] G. Nelin. A neutron diffraction study of palladium hydride. *physica status solidi (b)*, 45(2):527–536, 1971.

[101] Jacqueline M. Nicol, John J. Rush, and Richard D. Kelley. Inelastic neutron scattering studies of the interaction of hydrogen with palladium black. *Surface Science*, 197(12):67 – 80, 1988.

[102] Martin Nilsson and Steen Rasmussen. Cellular automata for simulating molecular self-assembly. In *DMCS*, pages 31–42, 2003.

[103] Masabumi NISHIKAWA, Tomofumi SHIRAISHI, and Kozo MURAKAMI. Solubility and separation factor of protium-deuterium binary component system in palladium. *Journal of Nuclear Science and Technology*, 33(6):504–510, 1996.

[104] M. Noureddine, R. Nassif, K. Saadouni, and Y.Boughaleb. Study of quenched impurities effect on order-disorder phase transition by monte-carlo method. *J. CONDENSED MATTER*, 2007.

[105] W. Oates and T. Flanagan. The reaction of hydrogen atoms with palladium and its alloys. *Canadian Journal of Chemistry*, 53(5):694–701, 1975.

[106] W A Oates and A M Stoneham. Strain-induced interaction energies between hydrogen atoms in palladium. *Journal of Physics F: Metal Physics*, 13(11):2427, 1983.

[107] WA Oates and Ted B Flanagan. Thermodynamic properties of regular interstitial solutions. *Journal of Materials Science*, 16(12):3235–3243, 1981.

[108] W.A. Oates, R. Lsser, T. Kuji, and Ted B. Flanagan. The effect of isotopic substitution on the thermodynamic properties of palladium-hydrogen alloys. *Journal of Physics and Chemistry of Solids*, 47(4):429 – 434, 1986.

[109] R. A. Oriani. The physical and metallurgical aspects of hydrogen in metals. *Unknown Journal*, 1993.

[110] P Orondo. Basic physics model for pdh thermodynamics. *preprint*, unknown.

[111] T. M. Ortiz, B. A. Meyer, and A. Razani. Empirical correlation of equilibrium separation factors in the pd-h2/d2 system with temperature and composition. *Journal of Chemical and Engineering Data*, 45(1):120–123, 2000.

[112] E. Pantos and J Bordas. Supercomputer simulation of small angle x-ray scattering, electron micrographs and x-ray diffraction patterns of macromolecular structure. *J.Pure and Appl. Chem. 66: 77-82*, 1994.

[113] A. Pendzig and W. Dieterich. Constant pressure simulations of lattice gas models. *J Chemical Physics*, 1996.

[114] J.K. Percus. Free energy, entropy, and lattice gas representations. *Physica A: Statistical Mechanics and its Applications*, 283(34):369 – 387, 2000.

[115] D.J. Picton, R.A. Bond, B.S. Bowerman, D.K. Ross, D.G. Witchell, I.S. Anderson, and C.J. Carlile. The influence of hh interactions on the phase diagram of pdh. *Journal of the Less Common Metals*, 88(1):133 – 140, 1982. International Symposium on the Properties and Applications of Metal Hydrides.

[116] MP Pitt and EM Gray. Tetrahedral occupancy in the pd-d system observed by in situ neutron powder diffraction. *EUROPHYSICS LETTERS*, 64(3):344–350, NOV 2003.

[117] D K Ross. Strong anisotropy in the inelastic neutron scattering from pdh at high energy transfer. *PHYSICAL REVIEW B*, 1998.

[118] J. M. Rowe, J. J. Rush, L. A. de Graaf, and G. A. Ferguson. Neutron quasielastic scattering study of hydrogen diffusion in a single crystal of palladium. *Phys. Rev. Lett.*, 29:1250–1253, Oct 1972.

[119] J. M. Rowe, J. J. Rush, J. E. Schirber, and J. M. Mintz. Isotope effects in the pdh system: Lattice dynamics of pdt$_{0.7}$. *Phys. Rev. Lett.*, 57:2955–2958, Dec 1986.

[120] J. M. Rowe, J. J. Rush, H. G. Smith, Mark Mostoller, and H. E. Flotow. Lattice dynamics of a single crystal of pdd$_{0.63}$. *Phys. Rev. Lett.*, 33:1297–1300, Nov 1974.

[121] M. Ruda, E.A. Crespo, and S. Ramos de Debiaggi. Atomistic modeling of h absorption in pd nanoparticles. *Journal of Alloys and Compounds*, 495(2):471 – 475, 2010. 15th International Symposium on Metastable, Amorphous and Nanostructured Materials.

[122] J. J. Rush, J. M. Rowe, and D. Richter. Dynamics of dilute h in beta-phase palladium deuteride: A novel mass defect. *Phys. Rev. B*, 31:6102–6103, May 1985.

[123] Y Sakamoto, M Imoto, K Takai, T Yanaru, and K Ohshima. Calorimetric enthalpies for palladium - hydrogen (deuterium) systems at h(d) contents up to about [h]([d])/[pd] = 0.86. *Journal of Physics: Condensed Matter*, 8(18):3229, 1996.

[124] E. Salomons. Elastic interaction of hydrogen in palladium studied by molecular-dynamics simulation. *Phys. Rev. B*, 42:1183–1188, Jul 1990.

[125] C San Marchi, B P Somerday, R S Larson, and F Rice S. Solubility of hydrogen and its isotopes in metals from mixed gases. *Journal of Nuclear Materials 372*, 2008.

[126] J. M. Sanchez and D. de Fontaine. Ordering in fcc lattices with first- and second-neighbor interactions. *Phys. Rev. B*, 21:216–228, Jan 1980.

[127] J. M. Sanchez, V. Pierron-Bohnes, and F. Mejía-Lira. Reciprocal-space analysis of short-range-order intensities by the cluster-variation method. *Phys. Rev. B*, 51(6):3429–3437, Feb 1995.

[128] A.B. Sazonov and .P. Magomedbekov. Concentration dependence of the separation factor of hydrogen isotopes in ternary and pseudoternary systems h2-h-x-y-h. *Atomic Energy*, 87(1):519–525, 1999.

[129] V. F. Sears and S. A. Shelley. Debye-waller factor for elemental crystals. *Acta Crystallographica Section A*, 47(4):441–446, Jul 1991.

[130] M. Shamsuddin. Hydrogen interaction in palladium alloys. *Journal of the Less Common Metals*, 154(2):285 – 294, 1989.

[131] Nobumitsu Shohoji. Statistical thermodynamic aspects of hydrogen in metals. *Surface and Coatings Technology*, 28(3):365–382, 1986.

[132] G Sicking, P Albers, and E Magomedbekov. Hydrogen isotope exchange and separation in gas-solid phase systems. *Journal of the Less Common Metals*, 89(2):373 – 391, 1983.

[133] Marcel Sluiter. Introducing distant interactions in the cluster variation method. *Computational Materials Science*, 2(2):293 – 300, 1994.

[134] S.Matar. Intermetallic hydrides: A review with ab initio aspects. *Progress in Solid State Chemistry*, 2010.

[135] L.I Smirnov and D.A Pronchenko. Chemical potential and phase diagrams of hydrogen in palladium. *International Journal of Hydrogen Energy*, 27(78):825 – 828, 2002. Proceedings of the Selected Papers of the Third International Con ference on Hydrogen Treatment of Materials, HTM-2001.

[136] B. Smit and D. Frenkel. Calculation of the chemical potential in the gibbs ensemble. *Molecular Physics*, 68(4):951–958, 1989.

[137] W Smith and M Lisal. Direct monte carlo simulation methods for nonreacting and reacting systems at fixed total internal energy or enthalpy. *Physical Review E 66*, 2002.

[138] T.Abbas and R.Khalil. Calculation of short range ordering in ni-ti alloys. *Unknown Journal*, 2005.

[139] M Tkacz and A Litwiniuk. Useful equations of state of hydrogen and deuterium. *Journal of Alloys and Compounds*, 2002.

[140] J. Tobochnik, H. Gould, and J. Machta. Understanding temperature and chemical potential using computer simulations. *Am. J. Phys*, 2005.

[141] A. van de Walle and G. Ceder. First-principles computation of the vibrational entropy of ordered and disordered pd_3V. *Phys. Rev. B*, 61:5972–5978, Mar 2000.

[142] G.H. Vineyard. Frequency factors and isotope effects in solid state rate processes. *J. Phys. Chem. Solids.*, 1957.

[143] Yan Wang, Sheng N. Sun, and M. Y. Chou. Total-energy study of hydrogen ordering in pdhx. *Phys. Rev. B*, 53:1–4, Jan 1996.

[144] C. T. White, D. W. Brenner, R. C. Mowrey, J. W. Mintmire, P. P. Schmidt, and B. I. Dunlap. D-d (h-h) interactions within the interstices of pd. *Japanese Journal of Applied Physics*, 30(Part 1, No. 1):182–189, 1991.

[145] E Wicke and J Blaurock. New experiments on and interpretations of hysteresis effects of pd-d2 and pd-h2. *Journal of the Less Common Metals*, 130(0):351 − 363, 1987.

[146] B. Widom. Some topics in the theory of fluids. *J. Chem. Phys*, 1963.

[147] T. Wieder. A generalized debye scattering formula and the hankel transform. *Zeitschrift Naturforschung Teil A*, 54:124–130, may 1999.

[148] T. Wieder. The debye scattering formula in n dimensions. *Journal of Mathematical and Computational Science*, 2:1086–1090, jun 2012.

[149] E. Wintersberger, D. Kriegner, N. Hrauda, J. Stangl, and G. Bauer. Algorithms for the calculation of x-ray diffraction patterns from finite element data. *Journal of Applied Crystallography*, 43(6):1287–1299, Dec 2010.

[150] Ralph J. Wolf, Myung W. Lee, Ricardo C. Davis, Patrick J. Fay, and John R. Ray. Pressure-composition isotherms for palladium hydride. *Phys. Rev. B*, 48:12415–12418, Nov 1993.

[151] K. Wyrzykowski and B. Baranowski. Pressure-concentration isotherms of pdhx thin films up to 0.2 gpa of gaseous hydrogen. *Journal of the Less Common Metals*, 141(1):73 − 81, 1988.

[152] W. Yen-Chang and J. Chen andS. Fang. Determination of curie temperature, short range order parameter and number of nearest neighbors of palladium atomes to iron atoms in palladium-iron alloys by resistivity measurement. *Chinese Journal of Physics, vol. 11, Issue 2, p.13*, 1973.

[153] X.W. Zhou, J.A. Zimmerman, B.M. Wong, and J.J. Hoyt. An embedded-atom method interatomic potential for pdh alloys. *Journal of Materials Research*, 23:704–718, 3 2008.

[154] Harald Zchner. Ewald wicke and his work on metal-hydrogen systems. *Journal of Alloys and Compounds*, 330332(0):2 – 7, 2002. Proceedings of the International Symposium on Metal-Hydrogen Systems, Fundamentals and Applications (MH2000).